

SIO-Mapper: A Framework for Lane-Level HD Map Construction Using Satellite Images and OpenStreetMap with No On-Site Visits

Younghun Cho¹ and Jee-Hwan Ryu^{1*}

Abstract—High-definition (HD) maps, particularly those containing lane-level information regarded as ground truth, are crucial for vehicle localization research. Traditionally, constructing HD maps requires highly accurate sensor measurements collection from the target area, followed by manual annotation to assign semantic information. Consequently, HD maps are limited in terms of geographic coverage. To tackle this problem, in this paper, we propose SIO-Mapper, a novel lane-level HD map construction framework that constructs city-scale maps without physical site visits by utilizing satellite images and OpenStreetmap data. One of the key contributions of SIO-Mapper is its ability to extract lane information more accurately by introducing SIO-Net, a novel deep learning network that integrates features from satellite image and OpenStreetmap using both Transformer-based and convolution-based encoders. Furthermore, to overcome challenges in merging lanes over large areas, we introduce a novel lane integration methodology that combines cluster-based and graph-based approaches. This algorithm ensures the seamless aggregation of lane segments with high accuracy and coverage, even in complex road environments. We validated SIO-Mapper on the Naver Labs Open Dataset and NuScenes dataset, demonstrating better performance in various environments including Korea, the United States, and Singapore compared to the state-of-the-art lane-level HD map construction methods.

Index Terms—Mapping, Image Processing, Neural Networks, Autonomous Vehicles

I. INTRODUCTION

ACCURATE vehicle localization is fundamental to most of autonomous driving algorithms such as path planning and control. However, these localization techniques mostly rely on High-Definition (HD) maps, which provide abundant semantic information including road topology, land topology, and traffic signs. Among the various information of HD maps, in this paper, we focus on lane-level HD maps, which offer precise lane information, which are particularly critical for vehicle localization methods.

However, lane-level HD map construction is currently limited to small geographic area due to the conventional methods that heavily rely on Mobile Mapping System (MMS) equipped with various sensors such as GPS, IMU, LiDAR, and cameras. MMS acquires highly accurate sensor data but require physical visit to the target areas. Additionally, even if sophisticated mapping algorithms such as a state-of-the-art SLAM algorithm integrates sensor data into maps, significant

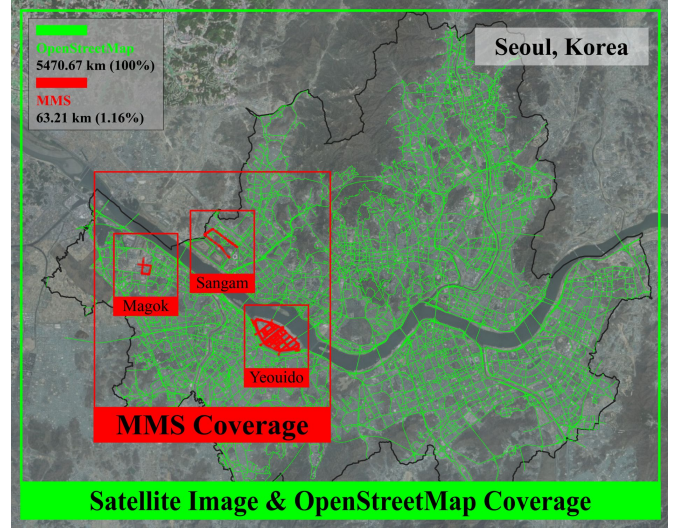


Fig. 1. Conventional lane-level HD maps only cover very limited portion of the entire road. For example, in Seoul which contains 5470.67 km of roads, only 63.21 km which is 1.16% of the road is covered as shown in this figure.

TABLE I
HD MAP COVERAGE IN SEOUL AND BOSTON

Region	Total Road Length (km)	HD map Coverage (km)	Ratio
Seoul	5470.67	63.21	1.16%
Boston	1504.22	21.91	1.46%

human intervention is required to assign semantic information such as road and lane topology. Consequently, lane-level HD map construction has been restricted to certain regions, and completed only by government agencies and large companies. For example, as shown in Fig. 1, Naver Labs Open Dataset and NuScenes provide lane-level HD map of Seoul and Boston seaport area but they only cover 63.21 kilometers and 21.91 kilometers which is about 1.16% and 1.50% of the entire road of each region as shown in Table I [1, 2].

Researchers have attempted to resolve two key challenges in lane-level HD map construction: automating the lane-level HD construction process to eliminate human intervention and constructing lane-level HD maps without visiting the target location from public data sources instead of utilizing sensor measurements obtained from the MMS. The first approach [3-15] focuses on methods that can extract lane-level information

¹Younghun Cho, and Jee-Hwan Ryu are affiliated with the Department of Civil and Environmental Engineering, KAIST, Daejeon 34141, Korea {dudgnsrj, jhryu}@kaist.ac.kr

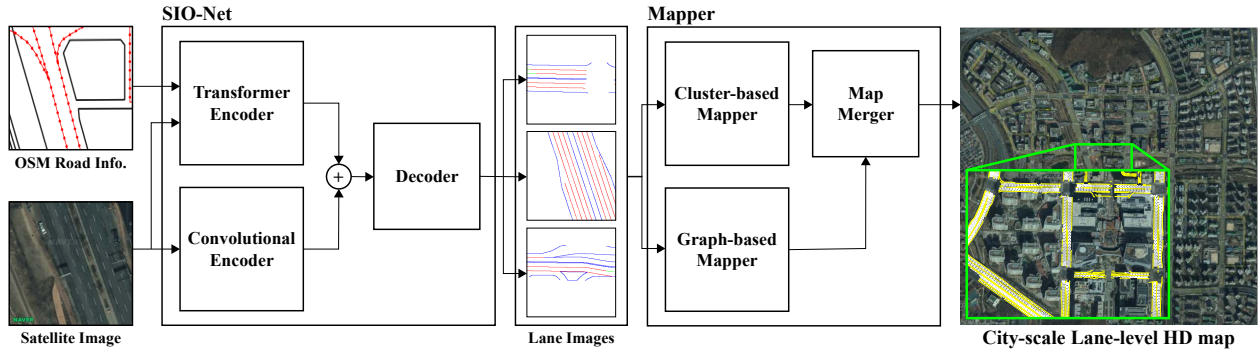


Fig. 2. Overall pipeline of the proposed SIO-Mapper. First, SIO-Net generate lane images. Transformer encoder and convolutional encoder each extract features in satellite images. Then, decoder concatenate both features and generate lane images. Then, mapper integrates lane images using cluster-based mapper and graph-based mapper and merge them using map merger to construct lane-level HD map. Using SIO-Mapper, we can construct a lane-level HD map in city-scale without any physical visit to the target area.

from sensor data collected by MMS. However, these methods often require costly, specialized equipment and are limited to the areas where sensors can be deployed, leading to restricted geographic coverage and high operational costs. On the other hand, the second approach [17-25] aims to construct lane-level HD maps using publicly available data, such as satellite images and OpenStreetMap (OSM), instead of on-site sensor measurements. While this method eliminates the need for physical site visits, existing techniques struggle to accurately stitch lane segments over large areas due to the lower resolution. Both approaches are still limited by the local scope of the maps they generate, as they rely on data with either narrow sensor range or incomplete coverage, making it difficult to construct seamless city-scale or global HD maps.

Even methods based on satellite imagery also suffer the same range limitation because high zoom levels are required to extract accurate lane information from the satellite imagery. These approaches struggle to integrate lane information over larger areas and only available to construct fragmented maps which lack the global context which are essential for city-scale autonomous driving. Moreover, most of conventional localization algorithms rely on comparing a query sensor measurement with reference maps, but existing HD maps construction methods do not offer comprehensive information in city-scale coverage. Therefore, a method that can overcome these geographic limitations is required to enable large-scale autonomous driving in real situations.

In this paper, we propose SIO-Mapper, a novel lane-level HD map construction framework designed to address these limitations. By utilizing publicly available satellite images and OpenStreetMap road data, SIO-Mapper constructs city-scale lane-level HD maps without requiring sensor measurements from physical site visit. SIO-Mapper improves lane-level HD map construction framework in two key modules as shown in Fig. 2. First, we propose SIO-Net, *Satellite Image* and *OpenStreetmap Network*, a deep learning network that extracts lane information more effectively than existing networks by combining Transformer-based encoders and convolutional encoders. SIO-Net utilizes OpenStreetMap road data to guide lane placement and extract detailed lane information from

satellite images which enables better lane extraction performance in both terms of accuracy and coverage. Second, we introduce a novel lane integration methodology that combines clustering-based and graph-based lane aggregation algorithms to merge lane segments across wider geographic areas. This approach addresses the limitations of merging lane segments in complex lane structures, ensuring the accurate lane-level HD map construction in city-scale. As a result, SIO-Mapper not only expands the coverage but also enhance the precision and usability of the lane-level HD maps, making it more effective for autonomous driving techniques in real situations. SIO-Mapper contributes in following three branches:

- **Enhanced Lane Extraction using SIO-Net**

We introduce SIO-Net, a novel deep learning network that outperforms existing lane extraction networks. Unlike existing methods, which often struggle with limited detail and precision, SIO-Net utilizes OpenStreetMap road data to guide the lane extraction by providing road shape into the network. Furthermore, the combination of Transformer-based and convolutional encoders enables to find complex structural patterns and fine-grained lane details, respectively. These improvements reduce lane extraction errors and enhance accuracy which are more suitable for the real-world road network.

- **City-scale Global HD Map Construction**

We also developed a city-scale lane-level HD map construction framework that overcomes the geographical limitation of existing mapping methods which are mostly restricted to the sensor's range. We achieve this by introducing a novel lane integration method that combines both clustering-based and graph-based methods. This approach selects only appropriate lanes for both methods, allowing for accurate lanes even in complex urban environments such as branching and merging lanes. The result offers significant improvements in both coverage and accuracy compared to existing methods. To the best of our knowledge, this is the first approach to construct a city-scale lane-level HD map without acquiring sensor measurements from physical site visit.

- **Standardized Lane-level HD Maps Evaluation Metrics**

Finally, we contribute to the field by providing evaluation metrics specifically designed for lane-level HD maps. Current evaluation methods often focus on pixel accuracy, which does not capture the performance of lane continuity and connectivity that is crucial in real-world autonomous driving scenarios. Our metrics evaluate the structural quality of lane connection and map coverage, offering a standardized benchmark for future research in this domain.

II. RELATED WORK

Lane-level HD map construction has actively researched with approaches broadly falling into two categories: automating lane-level HD map construction methods and lane-level HD map construction without visiting the actual site by utilizing public data sources.

A. Automating Lane-level HD Map Construction Methods

Researches to automate lane-level HD map construction began with synthesizing onboard sensor measurements and extracting lanes from them. Early approaches mostly utilized cameras as their main sensor and also utilized passive sensors such as GPS and IMU additionally. For example, Guo et al. integrated GPS and IMU data to extracted road segments based on the road network topology and accumulated bird-eye view (BEV) images to generate synthetic orthographic images of the segment. From those synthetic images, they finally extracted lane graph and validates localization performance using them [3, 4].

With the advent of LiDAR sensors, which provide dense 3D information, the momentum of research shifted from cameras to LiDAR. Gwon et al. accumulated ground points from LiDAR measurements using GPS and INS then extracted road markings by simple intensity threshold. They completed the lane map by interpolating road markings using B-spline algorithm [5]. Joshi and James additionally utilized OpenStreetMap (OSM) information as prior. They first extracted lane markings from LiDAR using intensity and aligned those lane markings into lines using RANSAC. Then, they performed particle filter along OSM nodes. Finally, by optimizing number of lanes as same as OSM information, they indexed the extracted lanes [6].

Then, research have advanced significantly with the development of deep learning networks. Liang et al. extracted road boundary from BEV LiDAR, BEV camera image, and elevation gradient derived from LiDAR using recurrent network named cSnake [7]. Similarly, Homayounfar et al. introduced DAGMapper, which extracts lanes in directed acyclic graph format from LiDAR intensity image, using three recurrent networks [8]. Zürn et al. additionally utilized semantic information. They introduced LaneGraphNet, which generate directional lane graph from BEV LiDAR, BEV camera image, vehicles and semantics, based on Graph-RCNN [9, 10]. Zhou et al. tried to complete lane graph by utilizing OSM information. They extracted lane using DeepLabv3+ [12] and particle filter, and then completed lane connection at intersections

using OSM road connecting topology [11]. Li et al. also suggested HDMaNet which construct local lane-level HD maps within sensor range of a LiDAR and six surrounding images and Liu et al. detect 3D lanes from pseudo BEV LiDAR image [13, 14]. Finally, Ort et al. introduced a remarkable HD lane mapping framework using OSM centerline information as prior. They extracted lanes using also DeepLabv3 and updated OSM centerline prior to complete lane-level HD map, which are considered as state-of-the-art method [15].

B. Lane-level HD Map Construction using Public Data Sources

To overcome the need for the physical visit of a MMS, researchers started to use satellite images which are publicly available and offer global coverage. Mátyus et al. segmented road and non-road area using ResNet [17] and generated road graph using A* algorithm [16]. Azimi et al. suggested Aerial LaneNet, FCNN-based neural network enhanced by Discrete Wavelet Transforms (DWTs). They outperformed existing algorithms in terms of pixel accuracy and Intersection over Union (IoU) [18]. However, Aerial LaneNet returns an output as rasterized image. However, rasterized lane images are difficult to construct maps in larger regions, as they are pixel-based information which cannot efficiently represent the continuous and interconnected road networks. Therefore, vectorized lane maps are required to maintain lane continuity and connectivity across wide regions.

From that perspective, He and Balakrishnan extracted lane-level street map using U-Net [20] with ResNet backbone. They divided and conquered this problem into non-intersection and intersection area. They first segmented lanes at non-intersection area and then connected them at intersections [19]. Xu et al. has tried to solve this problem across a series of papers. They first detected road curbs which is similar with road boundary using two approaches: suggesting connectivity-preserving loss for U-Net and adopting Feature Pyramid Network (FPN) [21, 22, 23]. Finally, they constructed city-scale road boundary by adding Attention for Adjacency Network (AfANet) after FPN to connect road boundaries by considering them as graph [24]. Also, they suggested RNGDet, which constructs road graph using Transformer [25, 26].

III. METHODOLOGY

To address these limitations, this section describes the detailed structure of proposed SIO-Mapper framework, which enables the city-scale lane-level HD map construction using publicly available satellite imagery and OpenStreetMap road information, without requiring physical visits to the target areas. SIO-Mapper framework consists of two main modules: SIO-Net for the lane extraction and the mapper for lane integration. The first module, SIO-Net, processes satellite images to extract lane segments using a combination of Transformer-based and convolution-based encoders. Transformer encoder leverages OpenStreetMap road information, embedding road shapes to guide the lane extraction process. By combining features from both encoders, SIO-Net generates lane images that contains both the structural and visual properties of the

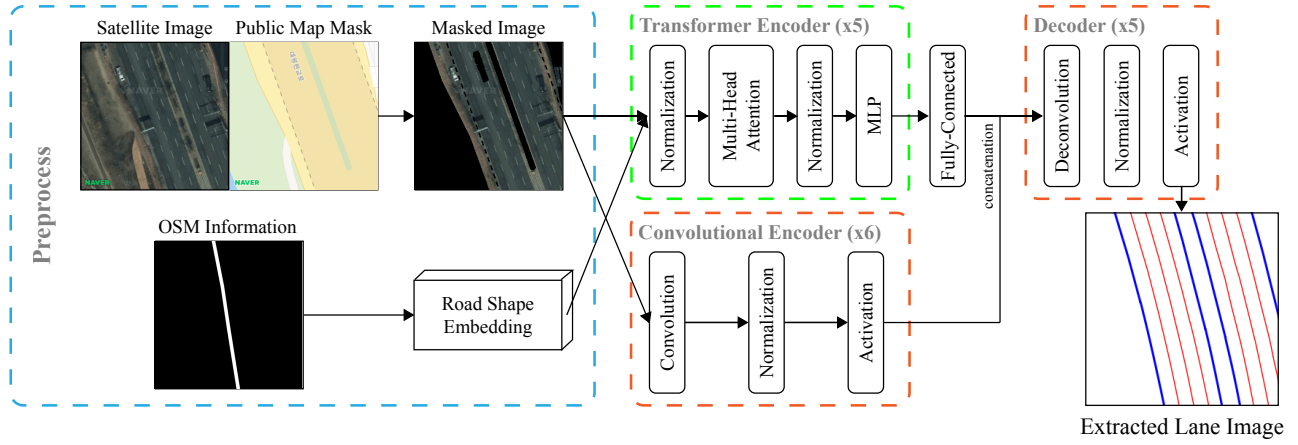


Fig. 3. This figure illustrates the pipeline of the suggested network, SIO-Net. In preprocess step, we mask the satellite image using public map mask and calculate road shape embedding by approximating the shape of road into quadratic function. Then, we extract image features using two different encoders, Transformer encoder and convolutional encoder, and concatenate both features. Finally, the decoder generate a lane image by decoding the concatenated feature. Lane image is consists of three labels which are respectively color coded in red, green, and blue: white broken lanes, white lanes, and yellow lanes.

road. The second module, mapper, integrates these extracted lane images into a lane-level HD map. This is achieved through a novel algorithm that combines advantages of clustering-based and graph-based stitching method. While clustering is effective in lane discrimination, graph-based method is effective for lane connectivity especially in complex road layouts. Unlike existing approaches which struggle with lane connectivity, the suggested method allows for the seamless merging of lane images by selecting lanes that are appropriate for both methods' criteria. By using Hungarian algorithm to optimize the lane stitching process, SIO-Mapper ensures seamless and accurate integration of lane images into cohesive, lane-level HD map that covers city-scale large geographic regions.

A. Problem Formulation

This paper focuses to construct lane-level HD maps without need for sensor-based site visits. Instead, we rely solely on publicly available data: satellite images and OpenStreetMap road information. These two data sources are complementary because OpenStreetMap provides global road network topology for wide areas, offering a structural skeleton, while satellite images offers detailed visual information for accurate lane extraction. The challenge lies in seamlessly combining these data to generate a coherent city-scale lane-level HD map. To achieve this, our framework first extracts lane images using SIO-Net, which is guided by the OpenStreetMap road shape information. The extracted lane images are then integrated using a novel mapper that ensures connectivity and accuracy by combining clustering-based and graph-based methods, resulting in a comprehensive city-scale lane-level HD map.

If represented as a formula, denoting satellite images $S = \{s_1, s_2, \dots, s_n\}$ with their center at interpolated road locations from OpenStreetMap as $X = \{x_1, x_2, \dots, x_n\}$, approximated road direction coefficients as $C = \{c_1, c_2, \dots, c_n\}$ and SIO-Net as $\phi(\cdot) = D(E_t(\cdot), E_c(\cdot))$, where $E_t(\cdot, \cdot)$, $E_c(\cdot)$, and $D(\cdot, \cdot)$ denote Transformer encoder, convolutional encoder, and decoder respectively, lane images $L = \{l_1, l_2, \dots, l_n\}$ are generated as $L_i = \phi(s_i, c_i)$. Then, the

mapper $M(M_c(\cdot), M_g(\cdot))$, where $M_c(\cdot)$ and $M_g(\cdot)$ denote clustering-based and graph-based mapper respectively, constructs a lane-level HD map G .

B. Lane Extraction using SIO-Net

To construct a reliable lane-level HD map, the lane extraction process should not only be highly accurate at the pixel level but should also maintain lane continuity and connectivity across the entire map. Therefore, we introduce SIO-Net, a novel deep learning network that combines both advantages of Transformer-based and convolutional neural networks as shown in Fig. 3. Transformer encoder focuses on connectivity of the road by embedding the road shapes provided by OpenStreetMap. Convolutional encoder, on the other hand, focuses on lane discrimination. By merging the output features of these two encoders, SIO-Net extracts lane images that are accurate in both terms of image accuracy and structural accuracy, addressing the critical need for lane continuity over city-scale areas.

1) *Preprocess*: In the preprocessing stage, we refine the satellite images to optimize the lane extraction process. To ensure the network focuses on relevant road areas, we filter out satellite images that do not contain any roads or lanes. Using OpenStreetMap data, we identify road locations and interpolate them at 1-meter intervals. Satellite images are then downloaded at these road points, with each image covering a 64m x 64m area at a resolution of 256 x 256 x 3 pixels. Also, because non-road area in satellite image also can interrupt the training, we mask the satellite image using public map downloaded at the same location.

Additionally, we preprocess the OpenStreetMap (OSM) road data, which is used as input to the Transformer encoder. To capture the road topology effectively, we approximate the shape of the roads using a quadratic function, which generates road shape coefficients. These coefficients are used as a road shape embedding in the Transformer encoder, providing structural guidance during the lane extraction process. This embedding acts as a reference to ensure that the extracted lanes align accurately with the underlying road topology, improving

the consistency and accuracy of lane extraction across various environments.

2) *Transformer Encoder*: Transformer encoder E_t extract features from satellite images based on Transformer and OpenStreetMap road information is used as road shape embedding. Transformer was originally designed as Large Language Model (LLM) which is specialized in calculating self-attention. Inspired by Transformer, we designed an encoder to calculate attention between image patches, so that patches that share same lane have a higher attention score. By using 4×4 image patch, $(256, 256, 3)$ image is transformed in $(4096, 784)$ shaped array and by adding three road topology coefficients C , the input shape becomes $(4099, 784)$.

Transformer encoder E_t is consist of five Transformer blocks. Because each Transformer block does not changes the shape of the input, an output feature f_t of the Transformer encoder E_t also has a shape of $(4099, 784)$.

3) *Convolutional Encoder*: Convolutional encoder E_c focuses on generating the accurate lane image L . In this module, we leveraged a conventional encoder structure consisting of convolution, normalization and activation functions.

Convolutional encoder E_c is consist of six encoder blocks with 16, 16, 32, 64, 128, and 256 feature dimensions and each block halves image size in both width and height. As a result, convolutional encoder returns an output feature f_c with a shape of $(256, 4, 4)$.

Because two encoders return features in different shape, we should match their shape before we feed them into the decoder. Using four convolutional layers that halve image size, a flatten layer, and a linear layer, we convert the output of Transformer encoder f_t to have the same shape, $(256, 4, 4)$, as output of the convolutional encoder f_c .

4) *Decoder*: Finally, decoder D generates a lane image L from two features f_t and f_c from each encoder. The decoder is consists of five decoder blocks. The first decoder block concatenates both features. From the second blocks, each block concatenates the output of the previous decoder block and the output of convolutional encoder block at the same level. Then, the concatenated tensor passes through a deconvolution layer that doubles image size, normalization layer, and activation layer. Each of them have 128, 64, 32, 16, and 3 feature dimensions which is the reverse of feature dimensions of convolutional encoder E_c .

C. Mapper

To complete the lane-level HD map G , we aggregated lane images L generated by SIO-Net. The most intuitive method to aggregate lane images is to convert lane images into lane points on the global coordinate system and cluster them. Clustering algorithms are powerful and efficient method to group lane points, however they have a crucial disadvantage that a point can only belong to only one cluster. As a result, clustering algorithm cannot perfectly discriminate lanes in specific conditions such as merging and diverging lanes. On the other hand, a graph-based methods are also can be adopted by considering each lane image as a graph and merging them. Graph-based methods can overcome the aforementioned

problem, however they heavily rely on hyperparameters and also need some heuristics. Therefore, we introduce a novel mapper that takes only advantages of both clustering-based and graph-based method.

1) *Clustering-based Mapper*: First, clustering-based mapper M_c starts with converting each lane image l_i into lane points $P = \{(x_1, y_1), (x_2, y_2), \dots, (x_n, y_n)\}$ using (1).

$$\begin{aligned} x_j &= x_i + p \cdot \left(P_x - \frac{w}{2} \right) \cdot \cos(\theta) \\ y_j &= y_i + p \cdot \left(P_y - \frac{h}{2} \right) \cdot \cos(\theta), \end{aligned} \quad (1)$$

where (x_j, y_j) denotes a global coordinate of each lane point, (x_i, y_i) denotes a global coordinate of image center which is road location from OpenStreetMap, p denotes pixel size in meter scale which is 0.25 m in this paper, (P_x, P_y) denotes a pixel coordinate of a lane point, (w, h) denotes image size, and θ denotes angle between image center and target pixel. Using this coordinate conversion, we generate lane points P_i that is according to each lane image l_i .

Then, we cluster lane points using DBSCAN [27] where each cluster represents each lane. In this module, we aggregate every lane points which belongs in same OSM road and cluster them at once.

$$\bar{P} = \cup_{i=1}^n P_i \quad (2)$$

$$DB(\bar{P}, 6, 10) = C = \{c_1, c_2, \dots, c_n\}, \quad (3)$$

where $DB(\cdot, \cdot, \cdot)$ denotes DBSCAN algorithm and each element denotes target points, minimum number of points, and maximum distance value used for clustering. Each cluster c_i represent lanes which are aggregated using clustering-based mapper. As a result, lane images L generate lanes $C = \{c_1, c_2, \dots, c_n\}$ in cluster form.

2) *Graph-based Mapper*: On the other hand, graph-based mapper first cluster lane points P_i in each lane image l_i using $DB(P_i, 4, 5)$. Then, we convert each lane image l_i into a graph g_i by assigning each lane cluster as a edge, and farthest point pairs of each cluster as start and end vertices of the lane. Then, we merge edges if their vertices are adjacent within 1 m. As a result, we get a graph $g_i = \{e_1, e_2, \dots, e_n\}$ which is composed of merged graph edges. Each edge e_j represent lanes which are aggregated using graph-based mapper. As a result, lane images L generate lanes $E = \{g_1, g_2, \dots, g_n\}$ in vectorized form.

3) *Map Merger*: Finally, we merge lane clusters C and lane graphs E to construct a lane-level HD map. Using the equation (III-C3), we find the cluster-edge pairs that maximizes the sum of the sharing points in each pair. This procedure enables to construct a global lane-level HD map that preserves both lane discrimination ability of clustering-based mapper and lane connectivity of graph-based mapper. By denoting the weight matrix ω , where $\omega(i, j)$ represents number of sharing lane points between lane cluster c_i and lane graph edge g_j , we maximize total number of sharing lane points using Hungarian algorithm as shown in following equations. Finding the permutation matrix P that maximizes the sum of the trace

TABLE II
INFORMATION OF DATASETS USED IN THIS EXPERIMENT

Dataset (Sequence)	NAVER LABS Open Dataset				NuScenes			
	Pangyo	Sangam	Yeouido	Magok	Boston	One North	Holland	Queens
# Road	111	101	189	110	164	720	263	341
# Road Points	18,299	11,571	24,718	15,117	22,201	20,941	9,074	12,083
Length (km)	20.32	15.24	31.81	16.16	21.91	25.56	11.98	16.16

of $P\omega$ has the exactly same physical meaning with finding the best pair that maximizes the sum of the sharing points.

$$\omega(i, j) = |C_i \cap E_j| \quad (4)$$

$$P = \operatorname{argmax}_P \sum \operatorname{Trace}(P\omega), \quad (5)$$

where permutation matrix P designate the cluster-edge pair $\tilde{P} = \{(\tilde{c}_1, \tilde{e}_1), (\tilde{c}_2, \tilde{e}_2), \dots, (\tilde{c}_n, \tilde{e}_n)\}$ that maximizes sharing lane points. Finally, we can construct a lane-level HD map $G = \{\tilde{c}_1, \tilde{c}_2, \dots, \tilde{c}_n\} = \{\tilde{g}_1, \tilde{g}_2, \dots, \tilde{g}_n\}$ that maximizes both advantages of clustering-based mapper and graph-based mapper. As a result, a global lane-level HD maps which have city-scale lane information can be constructed various environments using this framework as shown in V.

IV. EXPERIMENT

A. Benchmark Dataset

We validated our lane-level HD map construction framework on eight sequences from two datasets which provides HD lane information: Naver Labs Open Dataset [1] and NuScenes Dataset [2]. We directly utilized provided vectorized lane information as ground truth lane-level HD map and converted them into lane images and utilized as deep learning labels. Detailed information of datasets are described in Table II.

B. Comparison Method

To evaluate our suggested network, SIO-Net, we compared our result with HDMapNet[13], which is considered as state-of-the-art HD lane extraction algorithm, utilizing on-board sensor measurements: six surrounding images and one Li-DAR scan. By comparing with HDMapNet, we validated our suggested network shows comparable result with existing methods with only public data sources. However, because Naver Labs Open Dataset provides only four surrounding images, we revised the HDMapNet to use four images and trained the network again. Also, result of Yeouido sequence is not included because Naver Labs Open Dataset does not provide sensor measurements for the Yeouido sequence. Please note that SIO-Net distinguishes between three types of lanes, while HDMapNet extracts lanes indifferently.

On the other hand, to evaluate our suggested lane-level HD map construction framework, SIO-Mapper, we compared our resulting lane-level HD map with lane information provided by Naver Labs Open Dataset and NuScenes Dataset using after-mentioned lane-level HD map evaluation metrics we suggest.

C. Training Details

We sampled 69,705 satellite images that correspond to Naver Labs Open Dataset lane information. We utilized 55,764 images for training and 13,941 images for validation. We trained our suggested network on four Titan V GPUs over 10 epochs. On the other hand, HDMapNet was trained over 30 epochs with same condition for all other conditions.

Also, we adopted a loss function $L = L_R + L_S$, where L_R denotes reconstruction loss and L_S denotes semantic loss. For L_R , we used Binary Cross-Entropy (BCE) loss and for L_S , we introduced a novel semantic loss which represents the difference between the number of lanes in the label and number of clusters in generated lane image. This semantic loss function accelerates the training sequence by forcing each lane to become less blurred and clearer to match the number of lanes.

D. Lane-level HD map Evaluation Metrics

Evaluation lane-level HD maps, especially on a global scale, requires more than conventional metrics such as pixel accuracy and Mean Intersection over Union (mIoU), which are mostly used for image evaluations. These traditional metrics fall short when evaluating maps in vector format, where lane continuity and connectivity are crucial. To provide a comprehensive evaluation, we propose three new quantitative metrics specifically designed to assess the quality of vectorized lane-level HD maps.

Map Coverage (C_m): C_m indicates how much of the target mapping area is covered by the constructed lane-level HD map in a percentage. To match constructed lane-level HD map, \tilde{M} , and ground truth lane-level HD map, \tilde{G} , we utilized Hungarian method again.

This time, $\omega(i, j)$ denotes the distance between start and end vertices of \tilde{G}_i and \tilde{G}_j , where \tilde{G}_i and \tilde{G}_j represents edge i of \tilde{G} and edge j of \tilde{G} , respectively. By denoting $P' = P\omega$ and number of edges in \tilde{G} as $|\tilde{G}|$, we calculate a coverage of constructed lane-level HD map as shown in (6).

$$C_m = \frac{|\operatorname{Trace}(P') > 0|}{|\tilde{M}|} \times 100(\%) \quad (6)$$

On the other hand, we evaluate how accurate the map is using two criteria: map accuracy $A_m(\theta)$ and mean vertex distance D_v .

Map Accuracy ($A_m(\theta)$): First, accuracy is measured by how many lanes are constructed within the threshold compared to the ground truth. As shown in (7), we count number of edge pair previously bounded by Hungarian method and also calculate $A_m(\theta)$ in a percentage.

$$A_m(\theta) = \frac{P'(\theta)}{|\tilde{M}|} \times 100(\%), \quad P'(\theta) = |\operatorname{Trace}(P') < \theta| \quad (7)$$

Mean Vertex Distance (D_v): Finally, mean vertex distance, D_v , describes the actual distance, in meter scale, between the constructed lanes and ground truth lanes.

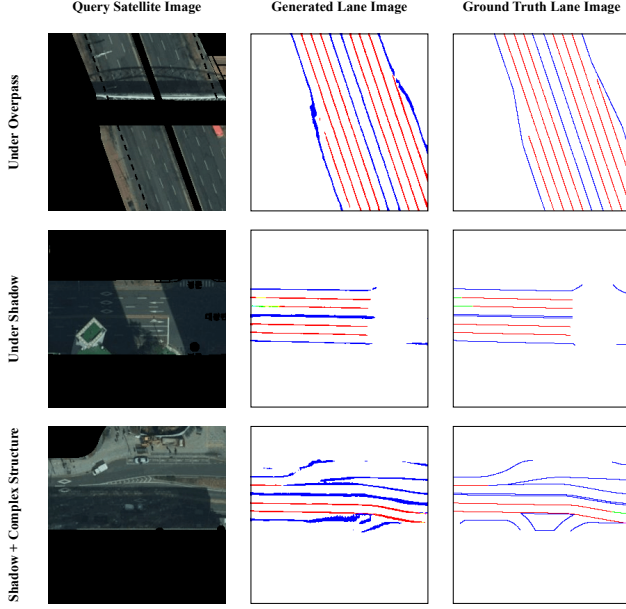


Fig. 4. Result at three challenging cases: under overpass, under shadow, and complex lane structure. Even a query image is partially blocked by diverse obstacle, OST still can generate lane image well. The last case, complex lane structure, does not perform perfectly, but they still perform properly except road boundary, where the vehicle actually drives.

$$D_v = \frac{\sum(Trace(P'))}{|Trace(P') > 0|} (m) \quad (8)$$

V. RESULTS

In this section, we present the result of the proposed method. First, we evaluate the lane extraction performance of our suggested network, SIO-Net, against to HDMapNet, which is considered as a state-of-the-art algorithm using on-board sensor measurements. Second, we evaluate the constructed lane-level HD map using SIO-Mapper using the suggested lane-level HD map evaluation metrics.

A. SIO-Net Evaluation

First, we evaluated SIO-Net on four sequences of Naver Labs Open Dataset. Fig. 4 illustrates three example cases in challenging environment: lanes under overpass, lanes under shadow, and a complex lane structure. As Fig. 4 shows, SIO-Net generates lane images with high accuracy even under challenging conditions. Table III details performance of SIO-Net compared to HDMapNet in terms of a pixel accuracy. Because HDMapNet does not discriminate types of lanes, we only calculated total pixel accuracy while we calculated pixel accuracy for each lane type for SIO-Net. Our proposed network performed better than HDMapNet utilizing only public data sources, achieving over 99% accuracy for each of the four sequences.

Table IV describes $mIoU$ of both SIO-Net and HDMapNet. As Table IV shows, SIO-Net achieved significantly lower $mIoU$ compared to both HDMapNet and pixel accuracy of SIO-Net. The reason for the low $mIoU$ is that lanes only take

TABLE III
PIXEL ACCURACY OF SIO-Net

Network	Lane Type	Pangyo	Sangam	Yeouido	Magok	Average
HDMapNet	Total	87.61%	91.85%	-	44.68%	74.71%
SIO-Net	White, Broken	99.23%	99.32%	99.38%	99.58%	99.38%
	White	99.85%	99.88%	99.89%	99.94%	99.89%
	Yellow	98.68%	98.60%	98.34%	98.83%	98.61%
	Total	99.26%	99.27%	99.20%	99.45%	99.30%

TABLE IV
 $mIoU$ OF SIO-Net

Network	Lane Type	Pangyo	Sangam	Yeouido	Magok	Average
HDMapNet	Total	0.8323	0.8788	-	0.4625	0.7245
SIO-Net	White, Broken	0.5533	0.5713	0.5147	0.4530	0.5231
	White	0.2542	0.3141	0.2357	0.1703	0.2436
	Yellow	0.4429	0.5031	0.4652	0.5023	0.4784
	Total	0.4168	0.4628	0.4052	0.3752	0.4150
Lane Ratio	Total	1.13%	1.34%	1.31%	0.95%	1.18%

TABLE V
EVALUATION OF GLOBAL HD LANE MAP

Network	Metric	Pangyo	Sangam	Yeouido	Magok	Average
HDMapNet	C_m	40.76%	30.27%	-	49.49%	40.17%
	$A_m(0.25)$	46.58%	11.73%	-	41.08%	33.13%
	$A_m(1.0)$	67.85%	36.90%	-	65.32%	56.69%
	$A_m(1.5)$	76.46%	48.81%	-	72.05%	65.77%
	D_v	0.3856 m	1.5724 m	-	0.4503 m	0.8028 m
SIO-Net	C_m	63.65%	67.33%	63.20%	73.18%	66.84%
	$A_m(0.25)$	54.11%	18.71%	20.25%	47.23%	35.08%
	$A_m(1.0)$	70.47%	52.08%	50.46%	75.74%	62.19%
	$A_m(1.5)$	77.01%	66.52%	60.93%	82.94%	71.85%
	D_v	0.2405 m	0.9416 m	1.0463 m	0.3568 m	0.6463 m

TABLE VI
EVALUATION USING GROUND TRUTH LANE IMAGES

Network	Metric	Pangyo	Sangam	Yeouido	Magok	Average
Naver Labs	C_m	83.07%	79.20%	75.21%	86.97%	81.11%
	$A_m(0.25)$	84.89%	64.06%	67.29%	85.71%	75.49%
	$A_m(1.0)$	91.90%	82.86%	85.81%	94.26%	88.71%
	$A_m(1.5)$	94.07%	88.82%	89.92%	95.73%	92.14%
	D_v	0.0588 m	0.1579 m	0.1563 m	0.0666 m	0.1099 m
		Boston	North	Holland	Queens	
NuScenes	C_m	92.08%	98.62%	92.66%	89.74%	93.28%
	$A_m(0.25)$	90.36%	97.45%	87.16%	85.08%	90.01%
	$A_m(1.0)$	93.42%	99.41%	90.21%	87.18%	92.56%
	$A_m(1.5)$	94.27%	99.41%	90.52%	87.65%	92.96%
	D_v	0.0743 m	0.0455 m	0.0659 m	0.0649 m	0.0627 m

a very small portion of the lane image, approximately 1%, as shown in the Table IV. While lanes in ground truth lane image perfectly have width of 1 pixel, lane images generated using deep learning network have thicker lanes. Therefore, union pixels becomes considerably larger than the intersection pixels and this phenomenon makes $mIoU$ smaller because $mIoU$ is calculated as intersection over union. However, in cluster-based and graph-based mapper, thicker lanes becomes a cluster and a graph edge so it does not effect to the resulting lane-level HD map.

B. SIO-Mapper Evaluation

Finally, we evaluate the lane-level HD map accuracy on four sequences of Naver Labs Open Dataset. We chose three threshold of map accuracy, A_m : 0.25 m, 1.0 m, and 1.5 m which represent the pixel resolution of the satellite image, half

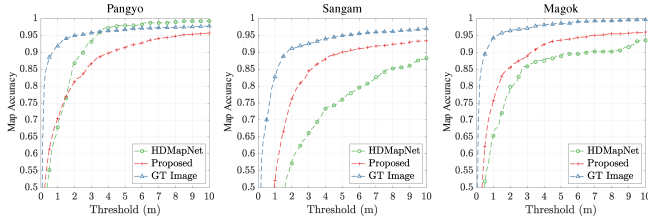


Fig. 5. Map accuracy, A_m , based on different thresholds for each sequence. Since the NAVER LABS Open Dataset does not provide LiDAR and camera data for the Yeouido sequence, there are no results using HDMapNet for the Yeouido sequence.

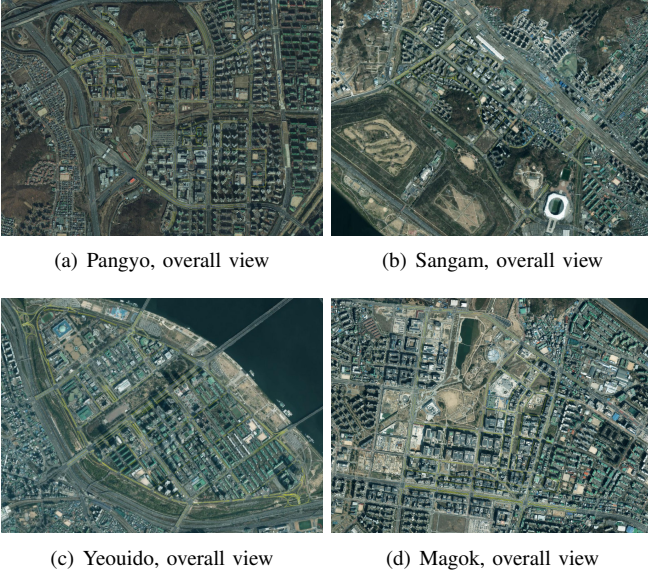


Fig. 6. Resulting city-scale lane-level HD maps for each sequences.

of the average vehicle size, and half of the average lane width, respectively. Depending on the purpose of the lane-level HD map, such as path planning and localization, users can choose different threshold values for suitable evaluation.

Table V details the quantitative evaluation of resulting lane-level HD maps in four sequences. As shown in the table, SIO-Net considerably outperforms HDMapNet even SIO-Net only utilizes OSM and satellite images while HDMapNet utilizes a LiDAR scan and six surrounding images. Also, suggested method shows mean vertex distance, D_v , 0.6463/m in average which is approximately 1/5 of the average lane width. However, as shown in Fig. 5, HDMapNet performs better when threshold is larger than 2 m in Pangyo sequence. This is occurred because SIO-Net totally failed in some road in Pangyo sequence.

Table VI shows the evaluation lane-level HD maps using ground truth lane images in eight sequences from two datasets. We compared it with the result using lane images generated from SIO-Net and HDMapNet to validate SIO-Net generates more proper lane images for the lane-level HD map construction. As the table shows, we guarantee over 83% of lanes generated with at least 64%, 82%, and 87% accuracy for each threshold using proposed framework. Also, we guarantee meter-level accuracy in terms of distance.

Also, the qualitative lane-level HD map construction result

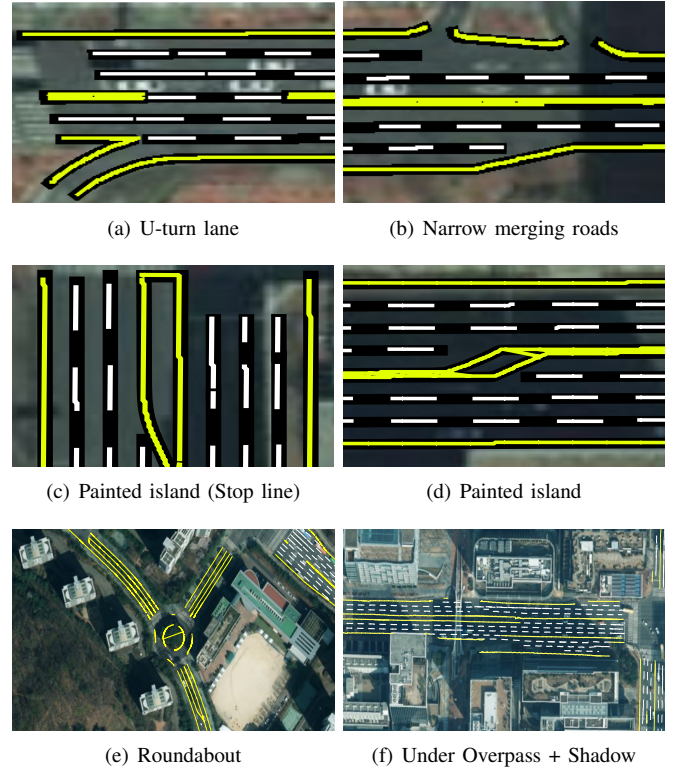


Fig. 7. Resulting lane-level HD map in various road environments. Black represents ground truth and colored lanes represent resulting lanes. (a): An example at the U-turn lane, where yellow and white lanes are mixed in one straight line. (b): An example at narrow merging roads with small yellow line fragments. (c), (d): Painted islands at the end of the road and middle of the road. (e): Roundabout with curved lanes. (f): Under overpass in urban environment with shadowed condition.

shows that our suggested framework SIO-Mapper constructs city-scale lane-level HD maps in various environments as shown in Fig. 6. Moreover, as shown in Fig. 7, SIO-Mapper constructs lane-level HD maps in challenging environments such as U-turn lanes, merging roads, painted islands, roundabouts, and overpasses.

VI. DISCUSSION AND CONCLUSION

In this paper, we successfully constructed city-scale lane-level HD maps, overcoming key limitations of previous approaches. SIO-Mapper framework not only eliminates the need of costly and time-consuming sensor-based physical visits but also achieves accurate lane-level HD maps in wide areas. To the best of our knowledge, this is the first fully automated approach that constructs a lane-level HD map from publicly available satellite images and OpenStreetMap road information, without requiring direct sensor measurements. Also, one of the major contributions of this paper is suggesting unified evaluation metrics specifically designed for vectorized lane-level HD maps. By introducing three new metrics, map coverage, map accuracy, and mean vertex distance, we provide comprehensive evaluation for both accuracy and coverage of lane-level HD maps. SIO-Mapper was validated across eight sequences from two datasets, demonstrating robust performance in diverse road environments with 87.20% map

coverage and 71.85% map accuracy at 1.5 m threshold on average.

However, there are still some limitations to address. SIO-Mapper heavily relies on the quality of the OpenStreetMap data and satellite images. Since OpenStreetMap is a crowd-sourced data, it may contain inaccuracies or outdated information, potentially affecting the resulting maps. Additionally, while satellite images are generally reliable, they are not updated frequently due to the high cost of satellite image acquisition. As a result, there can be mismatches between the satellite images and real-time road conditions. Future research should explore change detection and frequent updating of satellite images to ensure that the constructed HD maps remain accurate and up to date.

REFERENCES

- [1] “Naver labs open dataset: Hd map & localization dataset,” <https://www.naverlabs.com/datasets>, accessed: 2023-04-19.
- [2] H. Caesar, V. Bankiti, A. H. Lang, S. Vora, V. E. Liong, Q. Xu, A. Krishnan, Y. Pan, G. Baldan, and O. Beijbom, “nusenes: A multimodal dataset for autonomous driving,” in *CVPR*, 2020.
- [3] C. Guo, J.-i. Meguro, Y. Kojima, and T. Naito, “Automatic lane-level map generation for advanced driver assistance systems using low-cost sensors,” in *2014 IEEE international conference on robotics and automation (ICRA)*. IEEE, 2014, pp. 3975–3982.
- [4] C. Guo, K. Kidono, J. Meguro, Y. Kojima, M. Ogawa, and T. Naito, “A low-cost solution for automatic lane-level map generation using conventional in-car sensors,” *IEEE Transactions on Intelligent Transportation Systems*, vol. 17, no. 8, pp. 2355–2366, 2016.
- [5] G.-P. Gwon, W.-S. Hur, S.-W. Kim, and S.-W. Seo, “Generation of a precise and efficient lane-level road map for intelligent vehicle systems,” *IEEE Transactions on Vehicular Technology*, vol. 66, no. 6, pp. 4517–4533, 2016.
- [6] A. Joshi and M. R. James, “Generation of accurate lane-level maps from coarse prior maps and lidar,” *IEEE Intelligent Transportation Systems Magazine*, vol. 7, no. 1, pp. 19–29, 2015.
- [7] J. Liang, N. Homayounfar, W.-C. Ma, S. Wang, and R. Urtasun, “Convolutional recurrent network for road boundary extraction,” in *Proceedings of the IEEE/CVF Conference on Computer Vision and Pattern Recognition*, 2019, pp. 9512–9521.
- [8] N. Homayounfar, W.-C. Ma, J. Liang, X. Wu, J. Fan, and R. Urtasun, “Dagmapper: Learning to map by discovering lane topology,” in *Proceedings of the IEEE/CVF International Conference on Computer Vision*, 2019, pp. 2911–2920.
- [9] J. Zürn, J. Vertens, and W. Burgard, “Lane graph estimation for scene understanding in urban driving,” *IEEE Robotics and Automation Letters*, vol. 6, no. 4, pp. 8615–8622, 2021.
- [10] J. Yang, J. Lu, S. Lee, D. Batra, and D. Parikh, “Graph r-cnn for scene graph generation,” in *Proceedings of the European conference on computer vision (ECCV)*, 2018, pp. 670–685.
- [11] Y. Zhou, Y. Takeda, M. Tomizuka, and W. Zhan, “Automatic construction of lane-level hd maps for urban scenes,” in *2021 IEEE/RSJ International Conference on Intelligent Robots and Systems (IROS)*. IEEE, 2021, pp. 6649–6656.
- [12] L.-C. Chen, Y. Zhu, G. Papandreou, F. Schroff, and H. Adam, “Encoder-decoder with atrous separable convolution for semantic image segmentation,” in *Proceedings of the European conference on computer vision (ECCV)*, 2018, pp. 801–818.
- [13] Q. Li, Y. Wang, Y. Wang, and H. Zhao, “Hdmapnet: An online hd map construction and evaluation framework,” in *2022 International Conference on Robotics and Automation (ICRA)*. IEEE, 2022, pp. 4628–4634.
- [14] R. Liu, Z. Guan, Z. Yuan, A. Liu, T. Zhou, T. Kun, E. Li, C. Zheng, and S. Mei, “Learning to detect 3d lanes by shape matching and embedding,” in *Proceedings of the IEEE/CVF Winter Conference on Applications of Computer Vision*, 2023, pp. 4291–4299.
- [15] T. Ort, J. M. Walls, S. A. Parkison, I. Gilitschenski, and D. Rus, “Maplite 2.0: Online hd map inference using a prior sd map,” *IEEE Robotics and Automation Letters*, vol. 7, no. 3, pp. 8355–8362, 2022.
- [16] G. Mátyus, W. Luo, and R. Urtasun, “Deeproadmapper: Extracting road topology from aerial images,” in *Proceedings of the IEEE international conference on computer vision*, 2017, pp. 3438–3446.
- [17] K. He, X. Zhang, S. Ren, and J. Sun, “Deep residual learning for image recognition,” in *Proceedings of the IEEE conference on computer vision and pattern recognition*, 2016, pp. 770–778.
- [18] S. M. Azimi, P. Fischer, M. Körner, and P. Reinartz, “Aerial lanenet: Lane-marking semantic segmentation in aerial imagery using wavelet-enhanced cost-sensitive symmetric fully convolutional neural networks,” *IEEE Transactions on Geoscience and Remote Sensing*, vol. 57, no. 5, pp. 2920–2938, 2018.
- [19] S. He and H. Balakrishnan, “Lane-level street map extraction from aerial imagery,” in *Proceedings of the IEEE/CVF Winter Conference on Applications of Computer Vision*, 2022, pp. 2080–2089.
- [20] O. Ronneberger, P. Fischer, and T. Brox, “U-net: Convolutional networks for biomedical image segmentation,” in *Medical Image Computing and Computer-Assisted Intervention—MICCAI 2015: 18th International Conference, Munich, Germany, October 5–9, 2015, Proceedings, Part III 18*. Springer, 2015, pp. 234–241.
- [21] Z. Xu, Y. Sun, L. Wang, and M. Liu, “Cp-loss: Connectivity-preserving loss for road curb detection in autonomous driving with aerial images,” in *2021 IEEE/RSJ International Conference on Intelligent Robots and Systems (IROS)*. IEEE, 2021, pp. 1117–1123.
- [22] Z. Xu, Y. Sun, and M. Liu, “icurb: Imitation learning-based detection of road curbs using aerial images for autonomous driving,” *IEEE Robotics and Automation Letters*, vol. 6, no. 2, pp. 1097–1104, 2021.
- [23] T.-Y. Lin, P. Dollár, R. Girshick, K. He, B. Hariharan, and S. Belongie, “Feature pyramid networks for object detection,” in *Proceedings of the IEEE conference on computer vision and pattern recognition*, 2017, pp. 2117–2125.
- [24] Z. Xu, Y. Liu, L. Gan, X. Hu, Y. Sun, M. Liu, and L. Wang, “csboundary: City-scale road-boundary detection in aerial images for high-definition maps,” *IEEE Robotics and Automation Letters*, vol. 7, no. 2, pp. 5063–5070, 2022.
- [25] Z. Xu, Y. Liu, L. Gan, Y. Sun, X. Wu, M. Liu, and L. Wang, “Rngdet: Road network graph detection by transformer in aerial images,” *IEEE Transactions on Geoscience and Remote Sensing*, vol. 60, pp. 1–12, 2022.
- [26] A. Vaswani, N. Shazeer, N. Parmar, J. Uszkoreit, L. Jones, A. N. Gomez, Ł. Kaiser, and I. Polosukhin, “Attention is all you need,” *Advances in neural information processing systems*, vol. 30, 2017.
- [27] M. Ester, H.-P. Kriegel, J. Sander, X. Xu *et al.*, “A density-based algorithm for discovering clusters in large spatial databases with noise,” in *kdd*, vol. 96, no. 34, 1996, pp. 226–231.

VII. BIOGRAPHY



Younghun Cho received the B.S. degree in civil and environmental engineering from KAIST, Daejeon, Korea, in 2018, the M.S. degree in civil and environmental engineering from KAIST, Daejeon, Korea, in 2020, and the Ph.D. degree in civil and environmental engineering from KAIST, Daejeon, Korea, in 2024. Currently, he is an post doctoral researcher at Korea Institute of Machinery and Materials. His research interests include High-Definition mapping and LiDAR localization.



Jee-Hwan Ryu (Senior Member, IEEE) received the B.S. degree from Inha University, Incheon, South Korea, in 1995, and the M.S. and Ph.D. degrees from the Korea Advanced Institute of Science and Technology, Daejeon, South Korea, in 1997 and 2002, respectively, all in mechanical engineering. He is currently a Professor with the Department of Civil and Environmental Engineering, Korea Advanced Institute of Science and Technology. His research interests include haptics, telerobotics, exoskeletons, soft robots, and autonomous vehicles.